Published online 5 July 2012

Nucleic Acids Research, 2012, Vol. 40, No. 19 ***e151***
doi:10.1093/nar/gks651

Winding single-molecule double-stranded DNA on a nanometer-sized reel

Huijuan You[1,2], Ryota Iino[1,3], Rikiya Watanabe[1,3] and Hiroyuki Noji[1,3,*]

[1]Department of Applied Chemistry, School of Engineering, The University of Tokyo, Bunkyo-ku, Tokyo 113-8656, [2]Department of Biotechnology, Graduate School of Engineering, Osaka University, 2-1 Yamadaoka, Suita, Osaka 565-0871 and [3]CREST, Japan Science and Technology Agency, The University of Tokyo, Bunkyo-ku, Tokyo 113-8656, Japan

Received March 15, 2012; Revised May 28, 2012; Accepted June 12, 2012

ABSTRACT

A molecular system of a nanometer-sized reel was developed from F_1–ATPase, a rotary motor protein. By combination with magnetic tweezers and optical tweezers, single-molecule double-stranded DNA (dsDNA) was wound around the molecular reel. The bending stiffness of dsDNA was determined from the winding tension (0.9–6.0 pN) and the diameter of the wound loop (21.4–8.5 nm). Our results were in good agreement with the conventional worm-like chain model and a persistence length of 54 ± 9 nm was estimated. This molecular reel system offers a new platform for single-molecule study of micromechanics of sharply bent DNA molecules and is expected to be applicable to the elucidation of the molecular mechanism of DNA-associating proteins on sharply bent DNA strands.

INTRODUCTION

Many significant protein–DNA interactions involve sharp bending and looping of double-stranded DNA (dsDNA) with curvature radius of 2–20 nm (1). A remarkable example is the histone–DNA complex in eukaryotic cells; genomic dsDNA is wrapped around histone complexes with radii of 4.5 nm. The mechanistic properties of the histone–DNA complex is thought to be involved in the control of transcription activity (2). Most transcription factors also deform DNA by bending or looping DNA strands to regulate gene expression (3). DNA condensation occurs in extremely small viral capsids (radius of 15–50 nm) and is another example of extensive winding or bending of DNA (4). Thus, revealing the mechanical properties of dsDNA is crucial for understanding the molecular mechanisms of DNA–protein systems, and has been a focal issue in the physicochemical research on DNA (1).

Fundamental aspects of DNA bending mechanics have been studied using biochemical bulk measurements (5) and by pioneering single-molecule DNA stretching experiments (6,7). DNA bending is well described by the worm-like chain (WLC) model (8,9), in which the most important parameter is the persistence length, L_p, which characterizes the filament's resistance to thermal bending. The persistence length of DNA is reported to be ~50 nm for dsDNA, although the L_p of DNA changes depending on the experimental conditions and the DNA sequence used.

The single-molecule DNA stretching experiment has high versatility; it offers a unique experimental platform that allows one to study not only the mechanical properties of DNA but also the conformational dynamics of DNA associating proteins at the single-molecule level (10). Unidirectional motion of RNA polymerase or diffusive translocation of DNA-binding proteins along DNA strand were analyzed to elucidate their working principles.

However, DNA stretching experiments have limitations for the study of the micromechanics of sharply bent DNA or the molecular mechanism of DNA associating protein that induces DNA bending or binds to bent DNA. DNA stretching experiments typically measure the ensemble-averaged stiffness over a long DNA strand, in which small fragments may experience many small bending events influenced by thermal energy. Because thermal energy supplies only low forces in the order of ~0.1 pN (11), it is rarely possible to induce sharp bending of DNA with a curvature radius in nanometer range in DNA stretch experiments. Therefore, methodology that controls the bending curvature of DNA is required to explore the micromechanics of sharply bent DNA and its physiological role.

Several studies have been carried out to reveal the fundamental mechanical features of sharply bent DNA. Biochemical approaches, including DNA ligase-catalyzed cyclization experiments, have been used to quantitatively measure the ligation efficiency and circularization of short DNA fragments against bending force (12–14).

*To whom correspondence should be addressed. Tel: +81 3 5841 7252; Fax: +81 3 5841 1872; Email: hnoji@appchem.t.u-tokyo.ac.jp

These experiments allowed the estimation of the flexibility of DNA based on the ratio of the circularly-ligated to linearly-ligated fragments in a wide range of fragment lengths. Atomic force microscopy (AFM) provided more direct measurements of the distribution of dsDNA bending angles, allowing the estimation of the bending energy (15). However, immobilization of DNA on a surface for AFM imaging may have biased the populations of individual DNA forms. The direct measurement of bending force of dsDNA was also attempted by using a single-stranded DNA as a molecular force sensor, both ends of which were linked to the ends of bent dsDNA (16). However, the precision of the force determination suffered from the intrinsic noise and non-linearity of single-molecule Förster resonance energy transfer, on which this method relied on for the force estimation. It seems plausible that the WLC model fails to explain several results (12,13,15). Further investigation with regard to this issue is still necessary.

In this study, we developed a novel method to wind individual dsDNA molecules around the rotary motor protein F_1–ATPase (F_1) to directly measure the force and elastic energy required to bend dsDNA at nanometer-scale curvature radii. F_1 is the water-soluble portion of the F_oF_1–ATP synthase (Figure 1a) (17,18).

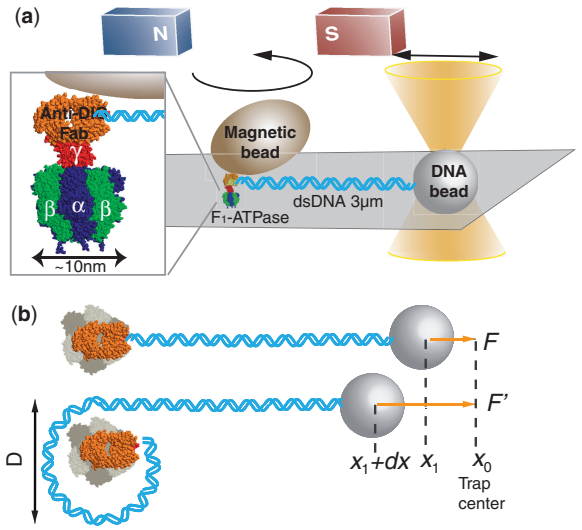

Figure 1. Experimental setup. (**a**) The molecular reel was constructed of F_1, a magnetic bead, and the Fab fragment on Ni–NTA glass. A biotinylated anti-DIG Fab fragment (orange) specifically linked the γ subunit (red) of F_1–ATPase and the streptavidin-coated magnetic bead. A dsDNA molecule (8.7 kb) was bridged between the anti-DIG Fab fragment and a streptavidin-coated polystyrene bead trapped using optical tweezers. The dsDNA was wound by rotating the magnetic bead using the magnetic tweezers. The stretching force was nearly parallel to the glass surface; the angle of the DNA strand against the coverglass was $<10°$. (**b**) The diameter of the wound DNA (D) was calculated from the total length of wound dsDNA (L) and the number of revolutions (n) as $D = L/n\pi$. The x_0 represents the center of the optical trap; x_1 and $x_1 + dx$ are the bead positions before and after winding. The length (L) of the wound dsDNA corresponds to the sum of the bead displacement (dx) and the increase of tethered dsDNA's extension (Supplementary Data). The winding tension (F) equals $k \cdot dx$ where k is the trap stiffness. Experiments were carried out at a low revolution rate (0.1 rps).

The minimum ATPase-active complex of the F_1 motor is the $\alpha_3\beta_3\gamma$ subcomplex, in which the γ subunit rotates against the $\alpha_3\beta_3$ stator in counterclockwise direction upon ATP hydrolysis (19). As a molecular reel for DNA winding, F_1 has an ideal size; the radius of the central shaft of the γ subunit is ~1 nm (radius of $\alpha_3\beta_3$ stator ring is ~5 nm), which is much smaller than the curvature radius of dsDNA loops induced by histones and transcription factors and thus suitable for winding dsDNA in freely suspended conditions. Our measurements showed that the curvature diameter of wound DNA decreased from 21.4 to 8.8 nm when tension was increased from 0.9 to 6.0 pN. The WLC model with the persistence length of 54 ± 9 nm well described our data, indicating that tightly bent dsDNA retained its structural integrity.

MATERIALS AND METHODS

DNA construct

The 8688 bp dsDNA was prepared by PCR using Ex-Taq DNA polymerase (TaKaRa, Japan) and the pRA100 plasmid as template (20). A 5′-biotin primer together with a 5′-digoxigenin (DIG) primer (Sigma Genosys, USA) were used in PCR reaction. PCR products were purified using the Wizard PCR clean-up system (Promega, USA). Purified DNA (12.5 μg) was incubated with 100 μl of streptavidin-coated polystyrene beads (0.5 μm diameter, 1% wt/vol, Bangs Laboratories, USA) suspension overnight, and unbound DNA was removed by washing several times using buffer (100 mM KPi, pH 7.0). The number of dsDNA strands bound to each bead was 1.7×10^2.

Protein preparation

A mutant of the $\alpha_3\beta_3\gamma$ subcomplex of F_1–ATPase from the thermophilic *Bacillus* PS3, $\alpha(His_6$ in N-terminus/$C193S)_3\beta(His_{10}$ in N-terminus$)_3\gamma(S108C/I211C)$, was expressed in *Escherichia coli* and purified as described previously (21,22) for the single-molecule rotation assay. Amino groups of the anti-digoxigenin (DIG) Fab fragment (Roche, Switzerland) were biotinylated with a 5-M excess of biotin–PEO–NHS (Pierce, USA) for 1 h at room temperature. After removing unreacted biotin–PEO–NHS using a spin column (Bio-Rad, USA), the remaining unreacted amino groups of the Fab fragment were reacted using an SPDP cross-linker (Pierce), which cross-links an amino group and a thiol group. After removing the unreacted cross-linker using a spin column (Bio-Rad), the SPDP-activated Fab fragment was reacted with cysteine residues that had been genetically introduced into the γ subunit of F_1 at a molar ratio of 1:3 (F_1 to Fab) overnight at room temperature. The biotinylated Fab–F_1 complex was stored at 4°C before use (Supplementary Figure S2).

Microscopy

An inverted microscope (IX71, Olympus, Japan) with a 100× objective lens (PlanSAPO NA1.3, Olympus), equipped with home-built magnetic tweezers (23) and

optical tweezers using an infrared laser (1047 nm, Nd:YLF, 1 W, IPG Photonics, USA), was used. Bright-field images were recorded using a CCD camera (MTI) at 30 frames/s and a high-speed camera (FASTCAM-1024PCI, Photron, USA) at 27 000 frames/s for winding experiments and calibration of trap stiffness, respectively. Bead position was measured as the centroid of the bright field image of the bead using Image J (National Institutes of Health, USA) and custom-made plug-ins (K. Adachi, Waseda University). Stiffness of the optical trap was estimated from the distribution of the *x*- and *y*-coordinates of the trapped bead. Trap stiffness was also measured from displacement of the trapped bead under the buffer flow, which exerted drag force on the trapped bead (Supplementary Data).

Construction of reel system

A 6-mm wide flow chamber was constructed from a Ni-NTA functionalized coverglass (32×24 mm^2) and an unmodified coverglass (18×18 mm^2) separated by two spacers ~50 μm thick. The bovine serum albumin (BSA) buffer (20 mM MOPS/KOH, pH 7.0, 50 mM KCl, 2 mM $MgCl_2$, 10 mg/ml BSA) was infused into the flow chamber. After a 5-min incubation to block non-specific protein binding, biotinylated Fab–F_1 (5 pM) in BSA buffer was infused into the chamber. After 15 min incubation, unbound F_1 was washed out of the chamber using BSA buffer. Next, streptavidin-coated magnetic beads (200–700 nm, Thermo Scientific, USA) in BSA buffer were infused into the chamber and incubated for 1 h. Unbound magnetic beads were removed with buffer. Finally, DNA-coated polystyrene beads (0.5 μm) in BSA buffer containing 2 mM ATP and 5 mM Biotin–PEG–NH_2 (MW3400, Creative PEG Works, USA) to block the non-specific binding of DNA to magnetic bead, were infused. The home-built magnetic tweezers were controlled using custom-made software (Celery, Library, Japan) (24). The *x*- and *y*-movements of the sample stage of microscope were manipulated using stepping motors (SGSP-13ACTR, Sigma Koki, Japan) controlled by custom-made software (ActOperator, Sigma Koki). Experiments were carried out at 25 ± 2°C.

RESULTS

Construction of reel system

The designed architecture of the molecular reel is shown in Figure 1a. The molecular reel to wind dsDNA was built using the F_1 molecule, a magnetic bead, and the Fab fragment (radius of ~2.5 nm) of the anti-digoxigenin (DIG) antibody. The anti-DIG antibody was covalently cross-linked to the γ subunit of F_1 and connected to the magnetic bead through biotin–streptavidin interaction. The complex of the γ subunit, anti-DIG Fab fragment, and the magnetic bead acted as a rotor while the $\alpha_3\beta_3$ stator was immobilized on the glass surface. dsDNA molecules of 8.7 kb labeled with DIG and biotin at distal 5′-ends were grabbed through the anti-DIG Fab fragment of the reel and a streptavidin-coated polystyrene bead that was trapped using optical tweezers.

Procedures for constructing the system were carried out as follows (Supplementary Figure S1). First, reel complexes were built by infusing the anti-DIG Fab–F_1 complex and magnetic beads solutions into a flow cell. The density of F_1 on the glass surface was maintained at <0.03 molecules/μm^2 (Supplementary Data). Some reel complexes showed continuous rotation at rotation speed faster than five revolutions per second (rps) in the presence of ATP (2 mM), indicating that the magnetic bead was tightly bound to the rotor γ subunit of a single F_1 molecule. Next, DNA-coated polystyrene beads, made of streptavidin-coated polystyrene beads and 5′-biotin and 5′-DIG labeled DNA molecules, were also introduced into the flow cell. A floating DNA-coated bead near a rotating F_1 molecule was captured and moved toward the rotating magnetic bead using optical tweezers until the DNA-coated bead inhibited the rotation of F_1 through steric hindrance. For establishing a connection between the 5′-DIG end of DNA and the anti-DIG Fab fragment on the rotor, the bead was held adjacent to the reel complex for 5–30 min. More than 340 experimental trials were conducted. Only 44 cases showed the connection of the DNA-coated bead to a rotating F_1 molecule. The connection was confirmed by observing that F_1 rotation was stalled when the stretching tension was exerted on DNA strand trapped with optical tweezers. In most of the failed cases, the DNA bead was simply not connected. In some cases, the DNA bead was anchored on a glass surface but at an apparently distant point from the rotation centre of the magnetic bead. These cases were omitted from the analysis. The experiment was often terminated by the detachment of the magnetic bead from glass surface, probably due to the detachment of His-tag or the dissociation of the γ subunit from the $\alpha_3\beta_3$ stator ring. Manipulation time before detachment was around 5–200 s. The released magnetic bead always accompanied the DNA-coated bead, which ensured the connection of the reel complex to DNA-coated bead.

Winding DNA with magnetic tweezers

After establishing the connection, the DNA molecule was stretched by horizontally moving the microscope stage using a stepping motor, and then an arbitrary level of tension was applied to the DNA strand to stall the ATP-driven rotation of F_1 (Figure 2). To minimize stage drift, the system was held for several seconds after applying the tension. Stage drift was typically within 10 nm per minute, which was measured using the polystyrene bead non-specifically attached on the glass in the same observation field or from the centroid of the rotating magnetic bead. Data exhibiting large drift were omitted from analysis. After holding the stage, the magnetic bead was rotated at 0.1 rps in a counterclockwise direction using the magnetic tweezers to wind the DNA. Upon winding, the polystyrene bead in the optical trap moved toward the rotating magnetic bead. In most cases, experiments were terminated due to detachment of the magnetic bead from glass surface as described before due to the developed tension. On detachment, the trapping force immediately decreased to zero (asterisk in Figure 2a and b).

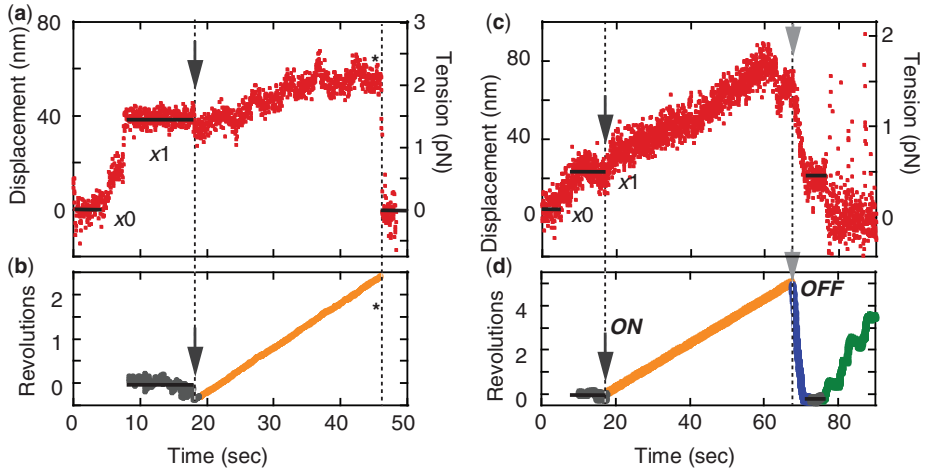

Figure 2. Time courses of winding experiments. (**a**) An example of the time course of the displacement of an optically trapped polystyrene bead during the winding procedure. Trap stiffness was 0.040 pN/nm. dsDNA was stretched at ~1.5 pN force for 8 – 18.5 s. (**b**) Time course of magnetic bead rotation during the winding experiment for (a). The magnetic bead was rotated from 18.5 s at 0.1 rps (orange line). The optically trapped bead was moved concomitantly with the magnetic bead rotation. After 2.5 revolutions, the magnetic bead detached from the glass surface (showed by asterisk). The optically trapped bead immediately returned to the trap center (x_0). (**c** and **d**) Time course of another winding experiment. Trap stiffness was 0.022 pN/nm. The magnetic bead was forcibly rotated for five revolutions. The optically trapped bead was constantly pulled toward the rotating magnetic bead. The sudden decrease at 63 s occurred for unknown reason; it might be due to structural relaxation of the DNA wound up around the molecular reel. The magnetic field was turned off at 66 s (gray arrowheads), and then, beads showed backward rotation (blue part). At 75 s, after reducing the tension exerted on DNA by moving stage, F_1 resumed ATP-driven rotation (green line).

In some cases, the system was able to withstand the stretching. When the magnetic tweezers were turned off (gray arrowheads in Figure 2c and d), the magnetic bead exhibited fast backward rotation, turning the same number of rotations as was observed in the forcible wind-up process. The speed of this backward rotation was 0.4–1.7 rps ($n = 3$). When the tension exerted on the molecular reel complex was completely removed by moving the stage, F_1 showed ATP-driven rotation (green data point in Figure 2d), indicating F_1 molecules were still active after manipulation. In some cases, F_1 did not resume ATP-driven rotation, likely due to the exposure of F_1 to infrared light for optical trapping. However, inactivated F_1 molecules still acted as molecular bearings; the magnetic beads showed rotational Brownian motion after the experiment (data not shown).

Winding tension versus curvature diameter

To draw a curve of winding tension (F) versus curvature diameter (D) of wound DNA, we determined the tension exerted on the DNA and the length of the DNA wound around the reel complex (L). The force was determined based on the displacement of the DNA-coated bead from the trap center of the optical tweezers. The stiffness of the optical tweezers used was 0.01 – 0.05 pN/nm (Supplementary Data). The diameter of wound DNA was calculated using $D = L/n\pi$; where n is the number of forced rotations. Because the displacement of the DNA bead upon winding was partly compensated by the increase of extension (dz) of the tethered DNA strand ($dz/L = 31-88\%$), the total length of the DNA wound around the reel complex (L) is equal to the sum of the displacement of DNA-coated bead (dx) and the increase of DNA extension (dz). Here, DNA extension was determined based on the force applied to the DNA in winding experiment, and the force–extension curve of the same DNA obtained from the stretching experiment (Figure 3a before correction, Figure 3b after correction). For precise measurement, only the data points from 1.0 to 2.0 revolutions were analyzed; data points of <1.0 or >2.0 revolutions did not provide reproducible values, likely due to the low precision of diameter estimation for <1.0 revolution and steric interactions between wound DNA strands for >2.0 revolutions.

Analysis of tension-diameter data with WLC model

Figure 4a shows the results of eight independent winding experiments represented by different colors, with winding tension ranging from 0.9 to 6.0 pN and curvature diameters ranging from 21.4 to 8.5 nm. Diameters were larger than the size of the nano-reel (~5 nm). Thus, this value represents the mechanical property of dsDNA without steric interaction with the reel. Based on the WLC model, the relationship between winding tension and loop diameter of dsDNA can be expressed as follows:

$$F = \frac{2\kappa}{D^2} = \frac{2L_p k_B T}{D^2} \quad (1)$$

where F is the winding tension, D is the curvature diameter of DNA loop, κ is the bending stiffness of dsDNA (also referred to as flexural rigidity), k_BT is thermal energy (4.1 pN•nm at room temperature) and L_p is the persistence length of dsDNA. By fitting the averaged data points of individual experiments (open squares in Figure 4a), L_p of sharply bent DNA was determined to be 54 ± 9 nm (mean ± standard deviation; correlation coefficient $R = 0.93$). This value agrees well with the previously reported persistence lengths from stretching experiments

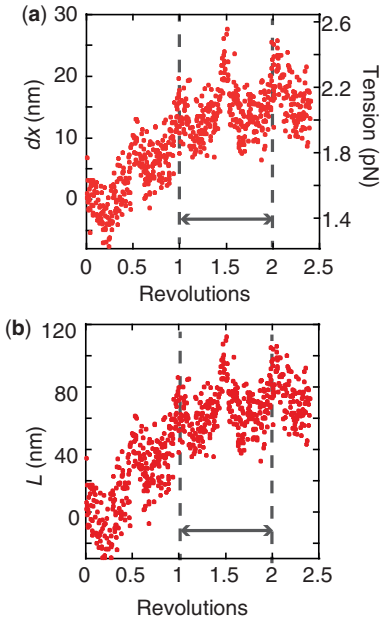

Figure 3. Wound DNA length versus revolutions. (**a**) Displacement of optically trapped bead (dx) versus revolutions (n). (**b**) Total length of wound dsDNA (L) versus revolutions (n). L was determined from dx and the force–extension curve of the same dsDNA (Supplementary Data). Considering the precision of dx determination or steric interaction with other wound DNA region, the data points between 1.0 and 2.0 revolutions were subjected to the data analysis (indicated by gray dashed line and arrow).

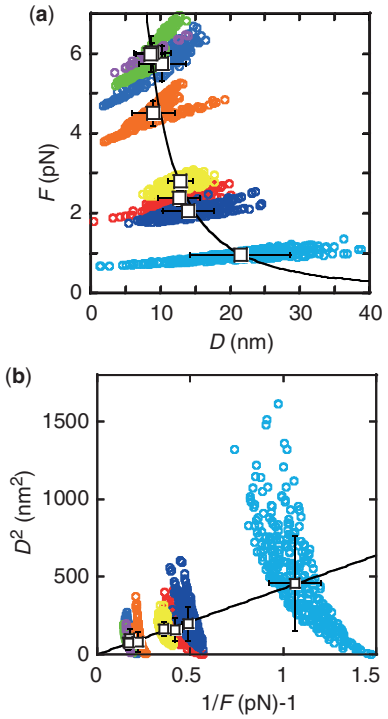

Figure 4. (**a**) Winding tension versus wound DNA diameter. Tension (F) versus diameter (D). Data points (n = 2027) were derived from eight individual measurements represented by different colors (open circles). Open squares represent the averaged values of each experimental trial, where the coefficient of variation (standard deviation/mean) for F was 4–13%, and for D was 14 – 35%. Black solid line is a fit of averaged data points with WLC model with Equation (1) and the fit parameter was L_p = 54 ± 9 nm (mean ± standard deviation). (**b**) The linear fit of D^2 versus $1/F$, corresponding to the WLC model (solid lines).

(~50 nm) (7). This agreement suggests that sharply bent dsDNA retains the same mechanical properties as dsDNA in the relaxed state, implying that deformation of dsDNA, such as local melting or kinking, does not occur under the present conditions. Based on our results, the force required to wind dsDNA into a circular loop with a curvature diameter of 9 nm, which represents the curvature diameter of dsDNA around a histone, is estimated to be 5.5 pN. The elastic energy (E) of a loop, calculated using the equation $E = 2L_p k_B T\pi/D$, is 38 $k_B T$.

DISCUSSION

We successfully wound single-molecule dsDNA around a nanometer-sized reel. As an application of this system, the mechanics of sharply bent dsDNA were studied. The results were consistent with the WLC model in the range of forces applied (0.9 – 6.0 pN). This finding agrees with the previous studies of the ligase-catalyzed cyclization experiments (14). However, there are also other studies reporting that dsDNA strands with curvature radius of 2 – 20 nm have higher flexibility than the WLC model predicts (12,13,15). The higher flexibility was attributed to a local melting bubble (25) or kink (26) formation during sharp bending (15). The reason for the discrepancy between this study and the previous works suggesting higher flexibility is unknown. One possible explanation is the difference in the DNA sequence. A recent cyclization experiment showed different DNA sequences had different persistence lengths (27) and short persistence length can explain the high flexibility. Recent theoretical study also showed that the sequence affect the tendency of DNA to form kinks. The GC-rich sequence is more flexible and kink formation can be observed when a GC-rich fragment is bent to curvature radius <2.4 nm (28). The sequence of DNA wound in our study has ~50% GC content and therefore kink would not be formed. To address this issue, a systematic study using dsDNA molecules with different sequences is required.

The present system for DNA winding at radii of a few nanometers offers a new platform for studying the molecular mechanism of DNA-associating proteins that bend or loop DNA. The enhancement of transcription factor's affinity to DNA was found by pre-bent DNA in a covalently closed circle (29). Our nano-reel system allows the systematic control of the curvature of wound DNA in wide range and in real time. By combining single-molecule imaging techniques such as fluorescence microscopy, the effect of DNA topology on the affinity of DNA-associating proteins can be directly studied.

Unlike synthetic polymers, the bending stiffness of dsDNA is extremely high due to the base pair stacking and the electrostatic effect. The elastic energy of a dsDNA molecule wound into a circle is approximately 50 times higher than that of single-strand DNA (ssDNA) (10). The high strain force of sharply bent dsDNA has been used to exert tension on enzyme

molecules to modulate catalytic activity (30). However, the lack of quantitative information regarding the mechanics of DNA molecules under high bending forces limits the application of dsDNA as a molecular spring in nanoengineering. We directly measured the restoring force of a wound DNA spring. Our method would provide a good calibration curve of the curvature radius and bending force for DNA spring work. In addition, it should be also emphasized that, to our knowledge, this is the first demonstration of the construction of a molecular reel system that can wind up a molecular wire and interconvert the linear motion and rotary motion. This technique could be also applicable for the development of molecular mechanical systems.

SUPPLEMENTARY DATA

Supplementary Data are available at NAR Online: Supplementary Information 1–4 and Supplementary Figures 1–5.

ACKNOWLEDGEMENTS

The authors thank M. Kino-oka (Osaka University), K. Hayashi (Tohoku University), and all members of the Noji laboratory for valuable comments and discussions and S. Nishikawa (Nikon, Japan) for technical support. Y.H. thanks the Ministry of Education, Culture, Sports, Science and Technology, Japan, and the International Graduate Program for Frontier Biotechnology, Graduate School of Engineering, Osaka University, for scholarship support.

FUNDING

Funding for open access charge: The Grants-in-aid for Scientific Research from Ministry of Education, Culture, Sports, Science and Technology (MEXT) [22247025 to H.N. and 23107720 to R.I.].

Conflict of interest statement. None declared.

REFERENCES

1. Garcia,H.G., Grayson,P., Han,L., Inamdar,M., Kondev,J., Nelson,P.C., Phillips,R., Widom,J. and Wiggins,P.A. (2007) Biological consequences of tightly bent DNA: the other life of a macromolecular celebrity. *Biopolymers*, **85**, 115–130.
2. Richmond,T.J. and Davey,C.A. (2003) The structure of DNA in the nucleosome core. *Nature*, **423**, 145–150.
3. Schultz,S.C., Shields,G.C. and Steitz,T.A. (1991) Crystal structure of a CAP-DNA complex: the DNA is bent by 90 degrees. *Science*, **253**, 1001–1007.
4. Jiang,W., Chang,J., Jakana,J., Weigele,P., King,J. and Chiu,W. (2006) Structure of epsilon15 bacteriophage reveals genome organization and DNA packaging/injection apparatus. *Nature*, **439**, 612–616.
5. Hagerman,P.J. (1988) Flexibility of DNA. *Annu. Rev. Biophys. Biophys. Chem.*, **17**, 265–286.
6. Smith,S.B., Finzi,L. and Bustamante,C. (1992) Direct mechanical measurements of the elasticity of single DNA molecules by using magnetic beads. *Science*, **258**, 1122–1126.
7. Wang,M.D., Yin,H., Landick,R., Gelles,J. and Block,S.M. (1997) Stretching DNA with optical tweezers. *Biophys. J.*, **72**, 1335–1346.
8. Vologodskii,A. (1994) DNA extension under the action of an external force. *Macromolecules*, **27**, 5623–5625.
9. Marko,J.F. and Siggia,E.D. (1995) Stretching DNA. *Macromolecules*, **28**, 8759–8770.
10. Bustamante,C., Bryant,Z. and Smith,S.B. (2003) Ten years of tension: single-molecule DNA mechanics. *Nature*, **421**, 423–427.
11. Bustamante,C., Smith,S.B., Liphardt,J. and Smith,D. (2000) Single-molecule studies of DNA mechanics. *Curr. Opin. Struct. Biol.*, **10**, 279–285.
12. Cloutier,T.E. and Widom,J. (2004) Spontaneous sharp bending of double-stranded DNA. *Mol. Cell*, **14**, 355–362.
13. Cloutier,T.E. and Widom,J. (2005) DNA twisting flexibility and the formation of sharply looped protein-DNA complexes. *Proc. Natl Acad. Sci. USA*, **102**, 3645–3650.
14. Du,Q., Smith,C., Shiffeldrim,N., Vologodskaia,M. and Vologodskii,A. (2005) Cyclization of short DNA fragments and bending fluctuations of the double helix. *Proc. Natl Acad. Sci. USA*, **102**, 5397–5402.
15. Wiggins,P.A., van der Heijden,T., Moreno-Herrero,F., Spakowitz,A., Phillips,R., Widom,J., Dekker,C. and Nelson,P.C. (2006) High flexibility of DNA on short length scales probed by atomic force microscopy. *Nat. Nanotechnol.*, **1**, 137–141.
16. Shroff,H., Reinhard,B.M., Siu,M., Agarwal,H., Spakowitz,A. and Liphardt,J. (2005) Biocompatible force sensor with optical readout and dimensions of 6 nm3. *Nano Lett.*, **5**, 1509–1514.
17. Boyer,P.D. (1997) The ATP synthase—a splendid molecular machine. *Annu. Rev. Biochem.*, **66**, 717–749.
18. Okuno,D., Iino,R. and Noji,H. (2011) Rotation and structure of FoF1-ATP synthase. *J. Biochem.*, **149**, 655–664.
19. Noji,H., Yasuda,R., Yoshida,M. and Kinosita,K. Jr (1997) Direct observation of the rotation of F1-ATPase. *Nature*, **386**, 299–302.
20. Aggeler,R., Chicas-Cruz,K., Cai,S.X., Keana,J.F. and Capaldi,R.A. (1992) Introduction of reactive cysteine residues in the epsilon subunit of *Escherichia coli* F1 ATPase, modification of these sites with tetrafluorophenyl azide-maleimides, and examination of changes in the binding of the epsilon subunit when different nucleotides are in catalytic sites. *Biochemistry*, **31**, 2956–2961.
21. Matsui,T. and Yoshida,M. (1995) Expression of the wild-type and the Cys-/Trp-less alpha 3 beta 3 gamma complex of thermophilic F1-ATPase in *Escherichia coli*. *Biochim. Biophys. Acta*, **1231**, 139–146.
22. Okuno,D., Fujisawa,R., Iino,R., Hirono-Hara,Y., Imamura,H. and Noji,H. (2008) Correlation between the conformational states of F1-ATPase as determined from its crystal structure and single-molecule rotation. *Proc. Natl Acad. Sci. USA*, **105**, 20722–20727.
23. Watanabe,R., Iino,R. and Noji,H. (2010) Phosphate release in F1-ATPase catalytic cycle follows ADP release. *Nat. Chem. Biol.*, **6**, 814–820.
24. Hirono-Hara,Y., Ishizuka,K., Kinosita,K. Jr, Yoshida,M. and Noji,H. (2005) Activation of pausing F1 motor by external force. *Proc. Natl Acad. Sci. USA*, **102**, 4288–4293.
25. Yan,J. and Marko,J.F. (2004) Localized single-stranded bubble mechanism for cyclization of short double helix DNA. *Phys. Rev. Lett.*, **93**, 108108.
26. Wiggins,P.A., Phillips,R. and Nelson,P.C. (2005) Exact theory of kinkable elastic polymers. *Phys. Rev. E Stat. Nonlin. Soft Matter Phys.*, **71**, 021909.
27. Geggier,S. and Vologodskii,A. (2010) Sequence dependence of DNA bending rigidity. *Proc. Natl Acad. Sci. USA*, **107**, 15421–15426.
28. Ortiz,V. and de Pablo,J.J. (2011) Molecular origins of DNA flexibility: sequence effects on conformational and mechanical properties. *Phys. Rev. Lett.*, **106**, 238107.
29. Parvin,J.D., McCormick,R.J., Sharp,P.A. and Fisher,D.E. (1995) Pre-bending of a promoter sequence enhances affinity for the TATA-binding factor. *Nature*, **373**, 724–727.
30. Zocchi,G. (2009) Controlling proteins through molecular springs. *Annu. Rev. Biophys.*, **38**, 75–88.